Journal of Materials Chemistry A

PAPER

View Article Online
View Journal | View Issue

Cite this: J. Mater. Chem. A, 2018, 6, 2767

Highly transparent tetraaminophthalocyanine polymer films for DSSC cathodes†

Kevin J. Klunder, C. Michael Elliott and Charles S. Henry *

Received 20th November 2017
Accepted 15th January 2018

DOI: 10.1039/c7ta10167h

rsc.li/materials-a

An inexpensive, transparent, catalytic, and highly stable material is the holy grail for a dye sensitized solar cell (DSSC) cathode. Despite a near exponential increase in research effort on DSSC cathodes, materials approaching this ideal have yet to be found. Transparent cathodes allow for front and back illumination of the solar cell, enable alternative anode materials and cell designs, and are important both for fundamental research and commercialization of DSSCs. In this work, thin polymeric films of nickel tetraminophthalocyanine (NiTAPc) were tested as a catalytic cathode material in Co(Bipy)-mediated DSSCs. The thin films are highly transparent with a transmittance at 550 nm (T550) of over 95% while maintaining an R_{ct} value below 1.3 Ω cm^2. The NiTAPc films are inexpensive, fast and easy to generate, and stable to 2000 cyclic voltammetry cycles. Long-term film stability was not realized, and a rise in the R_{ct} over time (days) occurred. However, poly-NiTAPc still represents one of the most transparent and catalytic materials reported to date. While historically phthalocyanines (Pc) have been studied as a dye/sensitizer, this first report of phthalocyanine use as a cathode material demonstrates they have utility on both sides of the DSSC.

Introduction

Since the inception of mesoporous dye sensitized solar cells (DSSC),[1,2] much attention has been placed on optimizing and understanding the anode and mediator components.[3,4] It has only been recently (past ~5 years) that significant effort has been made on cathode optimization, with a near exponential increase in new proposed cathode materials for both iodine and polypyridyl (and others)-based DSSCs.[5–8] Historically, platinum has been used as a catalyst to facilitate electron transfer at the cathode.[9–12] While the electron transfer kinetics with a platinum cathode are often sufficient for research purposes, the underlying cost is impractical for large scale production. Additionally, advances relating to increasing the efficiency of DSSCs have revealed that sluggish electron transfer and limited transparency at a platinum cathode can hinder the overall performance of a DSSC.[13–17] Noble metal cathodes, including gold, can also present stability problems due most likely to surface fouling.[18] Therefore, the lack lustre performance and high cost of noble metal cathodes has led to research into alternative materials. Graphene,[13–15,19] carbon nanotubes,[20–22] carbon nanofibers,[23] carbon black,[24] poly-aniline,[25,26] poly(3,4-ethylenedioxythiophene) (PEDOT),[27–31] and others,[32–34] have been proposed as cathode materials. However, new materials can be consuming to make and have elaborate fabrication methods, which could lead to elevated cost.[21,23,26] While many materials have been proposed, there remains a need for stable, cheap, highly transparent cathode materials.

A transparent cathode allows for bifacial solar cells,[35,36] a potential major advantage of DSSCs, in that nearly all angles of irradiance can generate photocurrent. Sequentially stacked DSSCs, which can enhance efficiency and tune voltage, are also possible with a clear cathode.[37] Transparent cathodes can also reduce the cost of DSSCs; a back illuminated DSSC can utilize less expensive anode substrates like Ti foil and stainless steel.[38] Additionally, by using substrates other than FTO, it leaves the option of growing TiO_2 films directly on the substrate with advanced control over morphology.[39,40] Transparent cathodes are also desirable to make colored photovoltaics for windows and consumer products.[41–43] Kavan detailed the need for a transparent highly catalytic cathode, with a focus on the transmittance at 550 nm (near the solar power maximum). The proposed optimal values are a charge transfer resistance of 1.3 Ω cm^2, and a 100% transmittance at 550 nm (T550).[6] Therefore, an inexpensive, stable material meeting these conditions would be the "holy grail" for a DSSC cathode.

Herein, we explore electrochemically polymerized nickel tetraaminophthalocyanine (NiTAPc) films as novel DSSC cathode materials. Phthalocyanines (Pcs) have a rich history in electrocatalysis due to their chemical stability, high activity, and low cost.[44,45] Pcs are used commercially in many applications such as data storage (CDs), paints, printing inks and tattoos.[46–48] More specifically, the use of metal tetraaminophthalocyanine-

Department of Chemistry, Colorado State University, Fort Collins, Colorado 80523-1872, USA. E-mail: chuck.henry@colostate.edu

† Electronic supplementary information (ESI) available. See DOI: 10.1039/c7ta10167h

modified electrodes are widely varied, were they have been shown to be useful in sensors, are electrochromic, and have possible energy storage applications.[49–53] Previous studies on polymeric tetraaminophthalocyanine films demonstrated them to be catalytic for a variety of electrochemical reactions.[50,51,54–56] More importantly, it has been reported that M-TAPc films have favourable electrochemistry towards ruthenium and cobalt tris(bipyridine) complexes.[57] However, in that work,[57] the conditions were not the same as those of a DSSC, nor were the electrochemical techniques used fully comparable to those found in current DSSC cathode research. The present study highlights conditions in a typical DSSC, as well as optimizing the NiTAPc films for a high transparency. Serendipitously, it was found that very thin layers of NiTAPc with a high transparency were the most catalytic, achieving a T550 of over 95% and R_{ct} below 1.3 Ω cm^{-2}. The findings imply that tetraaminophthalocyanines are an immediate candidate for use as back and front illuminated (bifacial) DSSCs, as well as opening the door for the use of a wide range of phthalocyanines as cathode materials in DSSCs.

Experimental

The electrochemistry was performed on a CHI-750 potentiostat. Polymerization was done in a 3-electrode cell with 2.5 cm^2 Pt counter and saturated calomel (SCE) reference electrodes. Electropolymerization was done starting at −0.1 and swept to 0.85 V, followed by a return scan, all at 100 mV s^{-1}. The polymerization solution was 2 mM NiTAPc (except Fig. 4) in dimethylsulfoxide (Alfa) with 0.1 M tetrabutylammonium hexafluorophosphate (Sigma).[52] The mediator was composed of 0.3 M $[Co^{2+}(Bipy)_3](PF_6)_2$, 0.055 M $[Co^{3+}(Bipy)_3](PF_6)_3$, 0.2 M $LiClO_4$ (Sigma), 0.2 M 4-*tert*-butylpyridine (TBP) (Sigma) in propylene carbonate (PC) (sigma) or acetonitrile (ACN) (Sigma). Two electrode cells used FTO (Sigma) or glassy carbon (Tokai) and a 25 μm Kapton spacer with working area 1 cm^2. AC impedance measurements were conducted from 0.1 to 10 000 Hz, at 0 V with perturbation amplitude of 10 mV. A Gamry EQCM 10 M was used to monitor mass changes, using a gold coated 10 MHz quartz crystal with a working area of 0.209 cm^2. X-ray photoelectron spectroscopy (XPS) was performed with a 5800 MultiTechnique XPS system, with Al Kα X-ray source. The high resolution spectra were fit with CasaXPS, using a Shirley background.

Nickel tetraaminophthalocyanine was synthesized using the phthalonitrile route, details can be found in the ESI.† NiTAPc characterization by ^{1}H-NMR, IR, and UV-Vis are in the ESI (Fig. S2–S4†). For UV-Vis measurements, a thin layer cell was used, with a 25 μm Kapton spacer and neat PC between two NiTAPc coated electrodes, bare FTO in the same configuration was used for background subtraction.

Results and discussion

Electropolymerization of NiTAPc

Initially, the polymerization of NiTAPc was examined on FTO (Fig. 1A), demonstrating the typical redox process previously

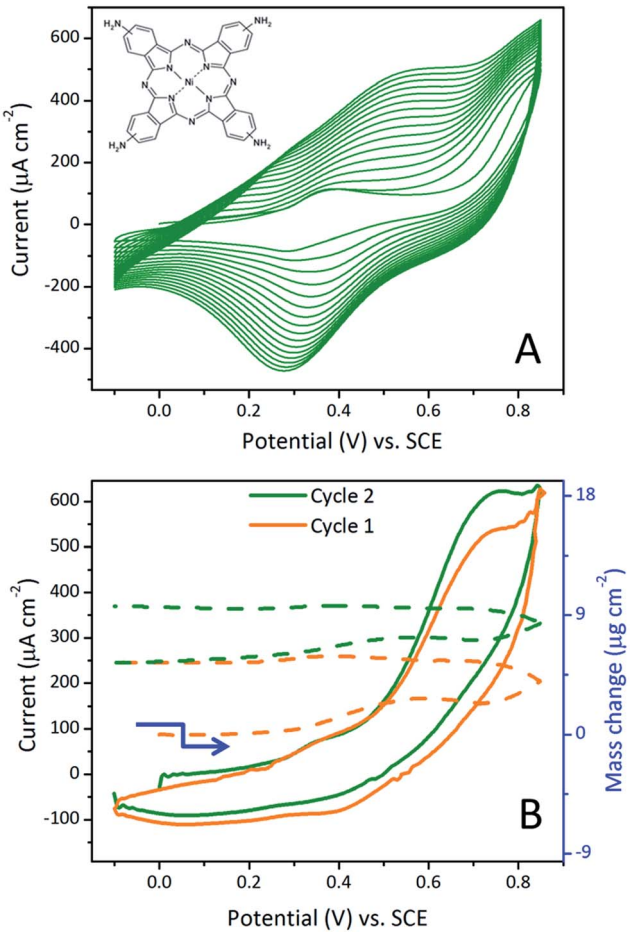

Fig. 1 (A) Electropolymerization of 2 mM NiTAPc in DMSO on a FTO electrode with 16 CV cycles. Inset shows the structure of NiTAPc monomer. (B) Polymerization of a 2-cycle film on a gold electrode with the use of an EQCM, dotted lines represent the right *Y*2 axis (blue).

reported for this polymer.[52] At ~0.25 V *vs.* SCE the $Ni^{3+/2+}$ couple is proposed, with oxidation of the amine functionalized ring occurring at ~0.7 V *vs.* SCE. Other redox process of the polymer are two ring reductions at −1.00 V and −1.45 V *vs.* SCE (not shown).[52] Upon cycling the electrode past ~0.7 V *vs.* SCE the formation of a conductive polymer occurs, with increasing current as a function of cycle number.[52]

Fig. 1B shows the deposition of the polymer as a function of current, with the use of EQCM to determine the mass change during polymerization.[58] Eqn (1) in the ESI† was used to relate frequency change to the mass change. On the initial anodic sweep (cycle 1), the first mass increase is speculated to be from ions or NiTAPc monomer adsorbed onto the electrode. The mass increase appears to start at the $Ni^{3+/2+}$ redox process at ~0.3 V *vs.* SCE, plateauing around ~0.65 V *vs.* SCE. Adsorption is likely at potentials less than 0.65 V *vs.* SCE since polymerization does not occur below this voltage.[52] The second mass increase event occurs above 0.65 V, most likely from polymerization. The mass increase is continued on the cathodic sweep until ~0.6 V where it plateaus. To our knowledge EQCM has not been used previously to examine the polymerization of NiTAPc,

however, the mass change events corroborate the earlier redox assignments for metal-TAPc electro-polymerization.[52]

Mass loading is related not only to electrode performance, but cost can be considered from the measured mass gained from EQCM experiments. Solvent, electrolyte, and porosity can all inflate the mass change seen in EQCM experiments of film growth,[59,60] however, they will be not accounted for here. If an assumption that only NiTAPc is being deposited on the electrode, ~6 μg cm^{-2} of material was deposited after the first cycle and ~4 μg cm^{-2} with the second cycle, for a total of 10 μg cm^{-2}. Using 10 μg cm^{-2}, the cost of a 2-cycle film was estimated to be \$0.65 m^{-2}. The material cost is based on synthetic cost of NiTAPc using retail sources and assumes a 50% yield. Additional details on cost analysis can be found in ESI (Table S1†). While the cost analysis is not all encompassing, as an estimate, it demonstrates that NiTAPc can be a potentially cost effective and scalable option as a polymeric coating for DSSC cathodes, as well as other catalytic electrochemical applications.

Charge transfer resistance to CoBipy

Upon successfully polymerizing NiTAPc and demonstrating the ability to adjust the mass and/or film thickness, the electrode coatings were investigated for their catalytic properties towards the popular Co(Bipy) DSSC mediator.[12] It was found that the charge transfer resistance increased with the number of deposition cycles, as shown in Fig. 2. The thin 2-cycle NiTAPc films gave R_{ct} values in the range of 0.5 Ω cm^2, with 2.3 Ω cm^2 for a 6-cycle film, and 23 Ω cm^2 for 16-cycle films. The 16-cycle film Nyquist plot cannot be fit with a simple Randles circuit. The spectra is better fit with two kinetically controlled processes, where a second charge transfer process is denoted here as R_{ct} (polymer). The additional charge transfer process is not uncommon in DSSC cathode research and it has been attributed to ionic mobility within the pores of PEDOT.[28] A similar second transfer process was also seen with a porous graphene coated FTO electrode.[15] An alternative explanation for the second charge transfer process may be from the rate of electron transport though the polymer matrix, which would scale with film thickness,[51] this has been seen with other polymeric catalytic coatings as well.[61] The calculated R_{ct} for the 16-cycle film is then the sum of R_{ct} (polymer) + R_{ct} Co(Bipy), and values of 9 Ω cm^2 and 14 Ω cm^2 were found, respectively.

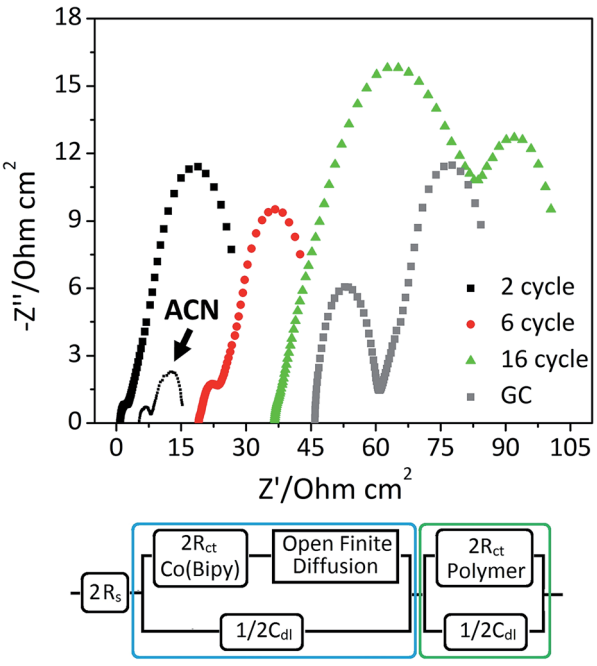

Fig. 2 Impedance spectra of Co(Bipy) in PC at glassy carbon (GC) modified with NiTAPc and bare GC. The 2-cycle film was also tested with Co(Bipy) in acetonitrile (ACN). (Bottom) The 2-cycle and 6-cycle NiTAPc modified electrodes are fit to a standard Randles circuit (blue outline). 16-cycle film was fit with the modified circuit which combines the green and blue outlines in the circuit diagram. Spectra are manually shifted on *X*-axis for clarity.

Propylene carbonate was chosen as the solvent to minimize evaporation during testing, but the data in Fig. 2 demonstrates that an R_{ct} using acetonitrile of 0.7 Ω cm^2 (2-cycle film) can be achieved. Acetonitrile is a popular solvent for testing DSSC's,[62] therefore the NiTAPc films should perform well in the solvent. The similar R_{ct} of PC and ACN is unusual as increased viscosity is typically related to slower kinetics with Co(bipy).[63] Perhaps the high Co(Bipy) and additive concentrations used here are causing deviations from previous observations for Co(bipy) in ACN and PC, where nearly an order of magnitude slower kinetics was seen in PC.[63] In any event, both higher viscosity PC (2.5 cP), and lower viscosity ACN (0.33 cP),[62] do not have vastly different charge transfer resistance to Co(bpy) in this system. Both solvents have an R_{ct} below the desired 1.3 Ω cm^2. Finally, the reproducibility of R_{ct} was briefly examined with the 2-cycle cells in PC, and a value of 0.67 ± 0.26 Ω cm^2 was found for 10 symmetric cells (20 electrodes total) over the period of one year. Overall, the lack of any highly specific set of optimized conditions to achieve R_{ct} values below 1.3 Ω cm^2 is promising (Fig. 4) for practical use of these coatings.

Polarization curves and Tafel plots of the symmetric cells used in Fig. 2 can be found in Fig. S5.† In a Tafel plot a steeper slope that approaches plateau sooner is indicative of fast kinetics,[24] this is seen with the 2-cycle and 6-cycle films. The 16-cycle and GC Tafel plots approached plateau with a slightly less steep slope, which agrees with the larger charge transfer resistance seen in Fig. 2. The fast kinetics of NiTAPc observed by EIS are then qualitatively corroborated with the Tafel plots.

Increased mass transfer resistance which can lower steady state current is seen with some DSSC counter electrode (CE) coating.[25] Therefore, measuring diffusion coefficients is important for CE characterization. Diffusion coefficients of Co(Bipy) were calculated with PC as the solvent. Values of 9.8 × 10^{-7} ± 1.2 × 10^{-7} cm^2 s^{-s} were calculated from the diffusion region in the Nyquist plots for all cells shown in Fig. 2 (details in ESI†). Diffusion coefficients were calculated a second way by using the limiting currents from the polarization curves in Fig. S5† and values of 6.2 × 10^{-7} ± 0.7 × 10^{-7} cm^2 s^{-s}. The polarization curves may be more accurate since they more resemble a working DSSC. As shown in Fig. S5† the 16-cycle film has a reduced limiting current, possibly from mass transfer resistances induced by the thicker film, further demonstrating

the enhanced performance of thinner NiTAPc films. Both methods for measuring diffusion coefficients gave values that are similar to previous reports of Co(Bipy) in PC.[63]

Optical transmittance and charge transfer resistance to Co(Bipy)

The polymer films were examined with UV-Vis spectroscopy to determine the relationship between transmittance and cycle number. Fig. 3 shows that the transmittance decreases with increasing cycle number, as expected. The transmittance of the NiTAPc films (Fig. 3) mimics the monomer spectra and has typical Q and Soret band absorption at 716 nm and 304 nm along with shoulders at 639 nm and 418 nm, respectively. The monomer UV-Vis spectra can be found in the ESI (Fig. S4†) and agrees quite well with a previous report for NiTAPc.[64] Additionally, the broadening of the peaks seen in Fig. 3 are typical of polymeric and layer-by-layer Pcs.[65,66] Interestingly, the thin films show an interference pattern from ~750 nm to 1000 nm that is indicative of a highly uniform coating.[67] Visually, the absorptions of poly-NiTAPc create a deep green color on the FTO substrate for thicker films (bottom Fig. 3). The 2-cycle NiTAPc film seems to have a less pronounced green appearance, probably from the thinner film having a more uniform transmittance from 300 nm to 900 nm. While the films are not fully transparent in the entire visible region, they are highly transparent at 550 nm near the solar spectrum power maxima (*Y*2 axis Fig. 3).[68]

In Fig. 4, the 1-cycle electrode made from 0.5 mM NiTAPc had a transmittance of 97.5% and R_{ct} of 1 Ω cm^2, which is very close to "the holy grail" values mentioned in the introduction. An apparent linear relationship is seen for the 2 mM condition,

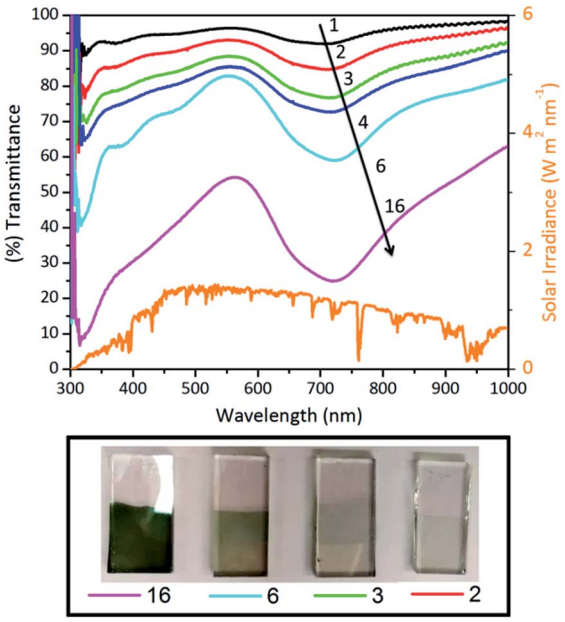

Fig. 3 Transmittance spectra of FTO coated with poly-NiTAPc with various cyclic voltammetry cycle numbers. The transmittance of FTO was subtracted. (Bottom) images of coated electrodes as a function of cycle number.

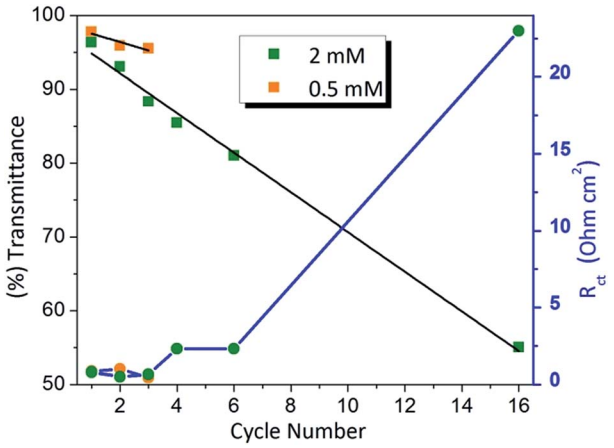

Fig. 4 Transmittance of NiTAPc films at 550 nm as a function of CV cycle. Charge transfer resistance is located on the *Y*2 axis. Circles are R_{ct} with blue connecting lines, squares are the transmittance with black lines as the linear fits.

and the linear fit was $Y = -2.7(\pm0.1)X + 97.5(\pm0.8)$ with an R^2 of 0.993. Since thin films appear to be the most catalytic and have the highest transmittance, a lower concentration was also tested to see if polymerization could be slowed down. The equation for the 0.5 mM condition was $Y = -1.2(\pm0.4)X + 98.7(\pm1)$, implying that (within error) the rate of film formation can be adjusted. Lower NiTAPc monomer concentrations may help with further optimization, whereby fine tuning the transmittance and R_{ct}.

Effect of 4-*tert*-butylpyridine on R_{ct} to Co(bipy)

4-*tert*-Butylpyridine (TBP) is a common additive to DSSCs,[69] but it has been shown to have deleterious effects on the charge transfer kinetics at the cathode.[18] While the kinetic effects of TBP are known at the anode (recombination),[69] it is rarely studied at the cathode. TBP effects are shown in Fig. 5 where the R_{ct} at glassy carbon increases from 9 Ω cm^2 to ~20 Ω cm^2 upon

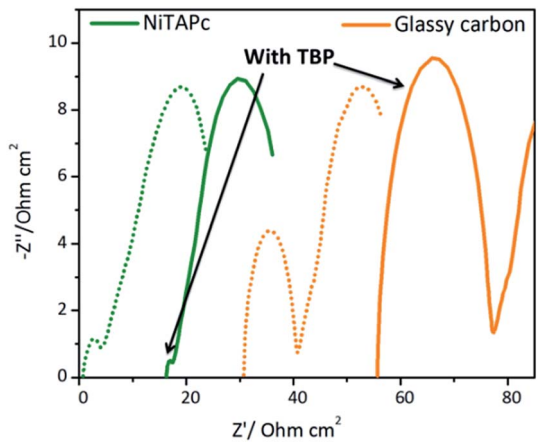

Fig. 5 Nyquist plots highlighting the effect of TBP on the charge transfer kinetics of 2-cycle NiTAPc modified and unmodified glassy carbon electrodes. Dotted lines are without TBP. Spectra are manually shifted on *X*-axis for clarity.

the addition of 0.2 M TBP. The increase may arise from adsorption of TBP to the carbon surface. McCreery has shown that a glassy carbon electrode contaminated with adventitious carbon can be cleaned with pyridine to improve kinetics, implying that pyridine strongly interacts with carbon surfaces.[70] In our work, the pyridine is never removed from the system, which may explain the different result. If adsorbed to the surface, TBP has an aliphatic moiety which would likely further hinder electron transfer. The opposite trend was seen for a glassy carbon electrode modified with a 2-cycle NiTAPc film. The NiTAPc-modified electrode had a nearly 60% decrease with R_{ct} with the addition of TBP. Apparently the TBP is not fouling the electrode in the same manor on NiTAPc films as it is with GC. Changing solvent dynamics with TBP may explain a lower R_{ct}. Murray,[63] as well as others,[71,72] have discussed various solvent effects for reaction rates of polypyridyl complexes, which can be related to ion-pairing, double layer effects, and viscosity. However, a detailed analysis of why TBP is lowering the R_{ct} will not be done here.

Stability of NiTAPc in CoBipy mediator solutions

The stability of catalytic coatings are of concern in DSSC applications given that the films are required to maintain catalysis over years of continued use.[73] Briefly, NiTAPc 2-cycle films were investigated for stability (Fig. 6). The 2-cycle NiTAPc films maintained excellent stability under cycling. After 2000 cycles, the R_{ct} value had a negligible increase from 0.4 to 0.6 Ω cm^2. However, in another set of experiments, after 24 h in mediator solution (ambient conditions), the R_{ct} value increased from 0.5 Ω cm^2 to 1.7 Ω cm^2, and on the fourth day climbed to 2.5 Ω cm^2. The stability over four days suggests that the NiTAPc films have some kinetically slow physical or chemical change within the polymer, which is increasing the R_{ct} value over time. It was thought that ambient oxygen was causing a change in the chemical structure of the NiTAPc films, however, stability experiments performed in oxygen free (≤1 ppm) drybox conditions gave similar results. The doping mechanism of metal-TAPc can change with the donor number of the solvent,[65] suggesting the slow change in R_{ct} could be related to the ion/solvent doping mechanism in PC. Related, remarkable stability of 1 million cycles has been reported for poly-aniline (a similar polymerizable moiety to NiTAPc) in ionic liquids,[74] attributed to a more reversible intercalation/doping mechanism. It is conceivable that a different solvent or electrolyte system may stabilize the NiTAPc polymer, whereby stabilizing the R_{ct} in a working DSSC. Solvent and electrolyte effects would make for a logical follow-up study to this initial work.

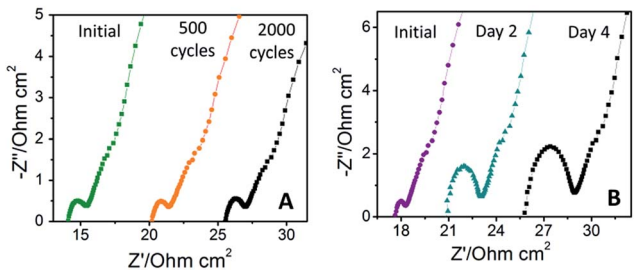

Fig. 6 (A) Impedance spectra of the 2-cycle films after repeated CV cycling at 400 mV s^{-1} from −0.5 to 0.5 V in DSSC mediator solution in a symmetric cell. (B) Spectra taken after days of aging in mediator solution. Spectra are manually shifted on *X*-axis for clarity.

XPS analysis of NiTAPc

To further examine the effects of cycling and aging on the NiTAPc films XPS measurements were performed. The "fresh" designation are for NiTAPc (2-cycle) films created about 1–2 h before XPS measurements. The "cycled & aged" films were left in mediator solution for 2 days, as well as cycled 1500 times. Fig. 7 has a representative survey spectrum for a NiTAPc 2-cycle film. The presence of tin in the spectra suggests that the NiTAPc film is only a few nanometers thick.

Interestingly, the spectrum lacks a fluorine signal that could arise from the substrate or the PF_6 electrolyte. Sulphur from DMSO was also not present. The only potential electrolyte present was chloride, possibly from the reference electrode or from lithium perchlorate. Not all the samples had measurable Cl, and the samples that did were ≤2 atomic%. A carbon to nitrogen ratio of 2.6 would be expected in pure NiTAPc, however, a ratio of ~5.2 was found in typical spectra. The difference is most likely from adventitious carbon. The bar graph in Fig. 7 shows that, within error, the Sn, N, C, and Ni elemental atomic% (from peak area) is not changing significantly for the two conditions. However, the O 1s atomic% does appear to be slightly increased for the aged films. This is examined further in the high-resolution spectra in Fig. 8.

The high resolution XPS collected for carbon, oxygen, tin and nitrogen are shown in Fig. 8. The shape of the C 1s and O

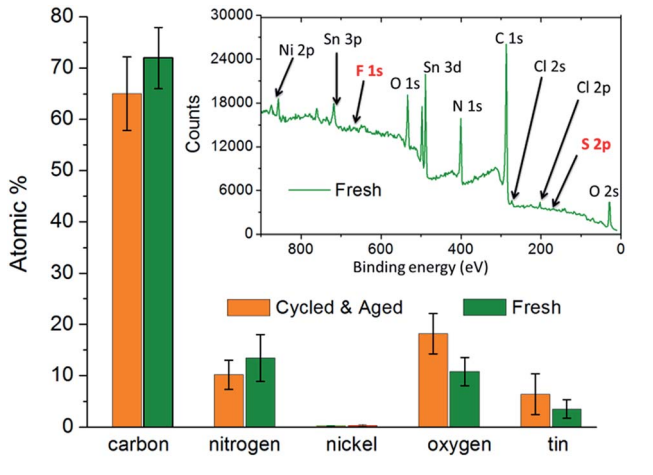

Fig. 7 Atomic percentage from XPS for NiTAPc (2-cycle) on FTO, and after aging for 2 days and cycled 1500 times. Nickel had a percentage of 0.32 ± 0.17% for fresh film and 0.24 ± 0.10% for the aged film. Error bars are from six individual electrodes for both conditions. Inset is a typical survey scan of a fresh 2-cycle NiTAPc film.

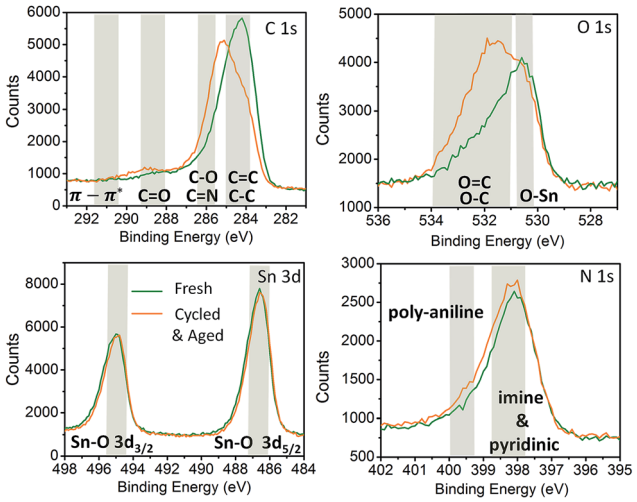

Fig. 8 Typical high resolution C, O, Sn, and N XPS of 2-cycle NiTAPc films on FTO before and after being cycled and aged. Grey bars represent general binding energies for specific chemical environments.‡

1s peaks change significantly with cycling, shifting to higher binding energies. One hypothesis for the peak shift could be that propylene carbonate has been incorporated into the polymer. PC incorporation would most likely raise the carbon%, however, this is not observed (Fig. 7). Alternatively, if NiTAPc was replaced by other carbon rich species, that would explain the different binding environments seen in Fig. 8. Related, in Fig. 7 it appears that on average the N and C content is lower for aged films, as well as increased Sn signal, somewhat supporting the loss of NiTAPc with aging hypothesis. Loss of material and polymer rearrangement is not unprecedented with N4 macro-cycles, were poly(tetraaminophenyl) porphyrin was reported to have a loss of oligomer/polymer material during aging & cycling.[75] If NiTAPc is lost, it may then be replaced by species from the mediator solution, or adventitious carbon.

Lost NiTAPc, if occurring, may expose surface hydroxyls on the FTO a possibly reason for the higher binding energies seen in the O 1s peak in Fig. 8.[76] Oxidative attack on the ring structure could be a possible explanation for the C 1s and O 1s peaks, but this seems unlikely since phthalocyanines are notoriously stable under ambient, as well as harsh, conditions.[48] Overall, there is no simple answer at the present for changes to the C 1s and O 1s peaks, none the less these chemical changes could be related to the instability of the poly-NiTAPc films. Finally, the nitrogen peak is changing very little, indicating the N binding environments are not drastically changing, this is promising because poly-NiTAPc are formed through amine linkages.

‡ The spectra of NiTAPc have been shifted by 1.2 eV as a correction to align the Sn 3d and O 1s peaks with known values for FTO. For FTO, Sn peaks occur at 495 eV for $3d_{3/2}$ and 486.5 eV for $3d_{5/2}$, and the O 1s in SnO_2 is at 530.5 eV.[77] General assignments for the O 1s,[78] N 1s,[79,80] and C 1s[78] are taken from previous literature precedent.

Conclusion

Phthalocyanines are introduced as new materials for cathodes in Co(bipy) mediated DSSCs. The thin NiTAPc films had an R_{ct} below 1.3 Ω cm^2 with a high transmittance at 550 nm of ~97%, representing a near ideal material for these two parameters. The cycling stability of the NiTAPc films was quite good, with only a 0.2 Ω cm^2 change in R_{ct} after 2000 cycles. The polymers lacked temporal stability over the course of four days, but only elevated to an R_{ct} of 2.5 Ω cm^2. The stability, activity and high transparency of the NiTAPc films makes these electrochemically formed polymers an immediate candidate for use in DSSC research in the area of back illumination. The present work also opens the door for phthalocyanines of all types for use as DSSC cathodes, in which adsorbed single layer or layer-by-layer films may be utilized, as well as the many (hundreds) other known phthalocyanine derivatives.

Conflicts of interest

The authors have no conflicts to declare.

Acknowledgements

This material is based on work supported by the National Science Foundation under grants to CSH (1710222) and CME (1058121). Any opinions, findings, and conclusions or recommendations expressed in this material are those of the author(s) and do not necessarily reflect the views of the National Science Foundation. This manuscript was also prepared posthumous to the loss of CME. Dr Elliott was an exceptional scientist, a steadfast friend, and a wonderful mentor. His loss was felt by the entire electrochemistry community.

References

1 B. O'Regan and M. Gratzel, *Nature*, 1991, **353**, 737–740.
2 A. Hagfeldt and M. Graetzel, *Chem. Rev.*, 1995, **95**, 49–68.
3 M. Grätzel, *J. Photochem. Photobiol., C*, 2003, **4**, 145–153.
4 S. Mathew, A. Yella, P. Gao, R. Humphry-Baker, B. F. E. Curchod, N. Ashari-Astani, I. Tavernelli, U. Rothlisberger, M. K. Nazeeruddin and M. Grätzel, *Nat. Chem.*, 2014, **6**, 242.
5 F. Hao, P. Dong, Q. Luo, J. Li, J. Lou and H. Lin, *Energy Environ. Sci.*, 2013, **6**, 2003–2019.
6 L. Kavan, J.-H. Yum and M. Graetzel, *Electrochim. Acta*, 2014, **128**, 349–359.
7 J. Theerthagiri, A. R. Senthil, J. Madhavan and T. Maiyalagan, *ChemElectroChem*, 2015, **2**, 928–945.
8 S. Yun, Y. Liu, T. Zhang and S. Ahmad, *Nanoscale*, 2015, **7**, 11877–11893.
9 M. K. Kashif, M. Nippe, N. W. Duffy, C. M. Forsyth, C. J. Chang, J. R. Long, L. Spiccia and U. Bach, *Angew. Chem., Int. Ed.*, 2013, **52**, 5527–5531.
10 G. Boschloo and A. Hagfeldt, *Acc. Chem. Res.*, 2009, **42**, 1819–1826.

11 S. Yanagida, Y. Yu and K. Manseki, *Acc. Chem. Res.*, 2009, **42**, 1827–1838.
12 S. A. Sapp, C. M. Elliott, C. Contado, S. Caramori and C. A. Bignozzi, *J. Am. Chem. Soc.*, 2002, **124**, 11215–11222.
13 L. Kavan, J. H. Yum and M. Grätzel, *ACS Nano*, 2011, **5**, 165–172.
14 L. Kavan, J.-H. Yum and M. Grätzel, *Nano Lett.*, 2011, **11**, 5501–5506.
15 L. Kavan, J.-H. Yum, M. K. Nazeeruddin and M. Grätzel, *ACS Nano*, 2011, **5**, 9171–9178.
16 S. Yun, A. Hagfeldt and T. Ma, *Adv. Mater.*, 2014, **26**, 6210–6237.
17 A. Hauch and A. Georg, *Electrochim. Acta*, 2001, **46**, 3457–3466.
18 L. N. Ashbrook and C. M. Elliott, *J. Phys. Chem. C*, 2014, **118**, 16643–16650.
19 H. M. Kim, I.-Y. Jeon, I. T. Choi, S. H. Kang, S.-H. Shin, H. Y. Jeong, M. J. Ju, J.-B. Baek and H. K. Kim, *J. Mater. Chem. A*, 2016, **4**, 9029–9037.
20 P. Dong, Y. Zhu, J. Zhang, F. Hao, J. Wu, S. Lei, H. Lin, R. H. Hauge, J. M. Tour and J. Lou, *J. Mater. Chem. A*, 2014, **2**, 20902–20907.
21 F. Hao, Z. Wang, Q. Luo, J. Lou, J. Li, J. Wang, S. Fan, K. Jiang and H. Lin, *J. Mater. Chem.*, 2012, **22**, 22756–22762.
22 J. E. Trancik, S. C. Barton and J. Hone, *Nano Lett.*, 2008, **8**, 982–987.
23 D. Sebastián, V. Baglio, M. Girolamo, R. Moliner, M. J. Lázaro and A. S. Aricò, *J. Power Sources*, 2014, **250**, 242–249.
24 I. P. Liu, Y.-C. Hou, C.-W. Li and Y.-L. Lee, *J. Mater. Chem. A*, 2017, **5**, 240–249.
25 H. Wang, Q. Feng, F. Gong, Y. Li, G. Zhou and Z.-S. Wang, *J. Mater. Chem. A*, 2013, **1**, 97–104.
26 J. Wu, Y. Li, Q. Tang, G. Yue, J. Lin, M. Huang and L. Meng, *Sci. Rep.*, 2014, **4**, 4028.
27 J. Idigoras, E. Guillen, F. J. Ramos, J. A. Anta, M. K. Nazeeruddin and S. Ahmad, *J. Mater. Chem. A*, 2014, **2**, 3175–3181.
28 B.-w. Park, M. Pazoki, K. Aitola, S. Jeong, E. M. J. Johansson, A. Hagfeldt and G. Boschloo, *ACS Appl. Mater. Interfaces*, 2014, **6**, 2074–2079.
29 H. N. Tsao, J. Burschka, C. Yi, F. Kessler, M. K. Nazeeruddin and M. Gratzel, *Energy Environ. Sci.*, 2011, **4**, 4921–4924.
30 W. Wei, H. Wang and Y. H. Hu, *Int. J. Energy Res.*, 2014, **38**, 1099–1111.
31 Y.-F. Lin, C.-T. Li and K.-C. Ho, *J. Mater. Chem. A*, 2016, **4**, 384–394.
32 M. J. Scott, J. J. Nelson, S. Caramori, C. A. Bignozzi and C. M. Elliott, *Inorg. Chem.*, 2007, **46**, 10071–10078.
33 G. Yue, J. Wu, Y. Xiao, M. Huang, J. Lin and J.-Y. Lin, *J. Mater. Chem. A*, 2013, **1**, 1495–1501.
34 F. Liu, S. Hu, X. Ding, J. Zhu, J. Wen, X. Pan, S. Chen, M. K. Nazeeruddin and S. Dai, *J. Mater. Chem. A*, 2016, **4**, 14865–14876.
35 A. Khan, Y.-T. Huang, T. Miyasaka, M. Ikegami, S.-P. Feng and W.-D. Li, *ACS Appl. Mater. Interfaces*, 2017, **9**, 8083–8091.
36 J. M. Miranda-Munoz, S. Carretero-Palacios, A. Jimenez-Solano, Y. Li, G. Lozano and H. Miguez, *J. Mater. Chem. A*, 2016, **4**, 1953–1961.
37 H. Cheema, R. R. Rodrigues and J. H. Delcamp, *Energy Environ. Sci.*, 2017, **10**, 1764–1769.
38 S. K. Balasingam, M. G. Kang and Y. Jun, *Chem. Commun.*, 2013, **49**, 11457–11475.
39 J. H. Park, Y. Jun, H.-G. Yun, S.-Y. Lee and M. G. Kang, *J. Electrochem. Soc.*, 2008, **155**, F145–F149.
40 P. Roy, S. Berger and P. Schmuki, *Angew. Chem., Int. Ed.*, 2011, **50**, 2904–2939.
41 C. J. M. Emmott, J. A. Rohr, M. Campoy-Quiles, T. Kirchartz, A. Urbina, N. J. Ekins-Daukes and J. Nelson, *Energy Environ. Sci.*, 2015, **8**, 1317–1328.
42 M. Saifullah, J. Gwak and J. H. Yun, *J. Mater. Chem. A*, 2016, **4**, 8512–8540.
43 Q. Tai and F. Yan, *Adv. Mater.*, 2017, **29**, 1700192.
44 J. H. Zagal, *Coord. Chem. Rev.*, 1992, **119**, 89–136.
45 J. H. Zagal, S. Griveau, J. F. Silva, T. Nyokong and F. Bedioui, *Coord. Chem. Rev.*, 2010, **254**, 2755–2791.
46 I. Schreiver, C. Hutzler, P. Laux, H.-P. Berlien and A. Luch, *Sci. Rep.*, 2015, **5**, 12915.
47 D. Dini and M. Hanack, *J. Porphyrins Phthalocyanines*, 2004, **08**, 915–933.
48 P. Gregory, *J. Porphyrins Phthalocyanines*, 2000, **04**, 432–437.
49 H. Li and T. F. Guarr, *J. Electroanal. Chem. Interfacial Electrochem.*, 1991, **297**, 169–183.
50 H. Li and T. F. Guarr, *Synth. Met.*, 1990, **38**, 243–251.
51 H. Li and T. F. Guarr, *J. Electroanal. Chem. Interfacial Electrochem.*, 1991, **317**, 189–202.
52 H. Li and T. F. Guarr, *J. Chem. Soc., Chem. Commun.*, 1989, 832–834.
53 A. Sivanesan and S. A. John, *Biosens. Bioelectron.*, 2007, **23**, 708–713.
54 Z.-H. Wen and T.-F. Kang, *Talanta*, 2004, **62**, 351–355.
55 Z. Sun and H. Tachikawa, *Anal. Chem.*, 1992, **64**, 1112–1117.
56 Q.-Y. Peng and T. F. Guarr, *Electrochim. Acta*, 1994, **39**, 2629–2632.
57 H. M. Xi and F. A. Schultz, *J. Electroanal. Chem.*, 1993, **361**, 49–56.
58 A. R. Hillman, *J. Solid State Electrochem.*, 2011, **15**, 1647–1660.
59 S. J. Martin, V. E. Granstaff and G. C. Frye, *Anal. Chem.*, 1991, **63**, 2272–2281.
60 R. Schumacher, G. Borges and K. K. Kanazawa, *Surf. Sci.*, 1985, **163**, L621–L626.
61 Y. V. Ulyanova, A. E. Blackwell and S. D. Minteer, *Analyst*, 2006, **131**, 257–261.
62 J. Wu, Z. Lan, J. Lin, M. Huang, Y. Huang, L. Fan and G. Luo, *Chem. Rev.*, 2015, **115**, 2136–2173.
63 R. Pyati and R. W. Murray, *J. Am. Chem. Soc.*, 1996, **118**, 1743–1749.
64 T. Mugadza and T. Nyokong, *Electrochim. Acta*, 2010, **55**, 6049–6057.
65 N. M. Alpatova, E. V. Ovsyannikova, L. G. Tomilova, O. V. Korenchenko and Y. V. Kondrashov, *Russ. J. Electrochem.*, 2001, **37**, 1012–1016.

66 Y. Açıkbaş, M. Evyapan, T. Ceyhan, R. Çapan and Ö. Bekaroğlu, *Sens. Actuators, B*, 2007, **123**, 1017–1024.
67 R. Swanepoel, *J. Phys. E: Sci. Instrum.*, 1983, **16**, 1214.
68 *ASTM G173-03 Reference Spectra Derived from SMARTS v. 2.9.2*.
69 T. M. Koh, K. Nonomura, N. Mathews, A. Hagfeldt, M. Grätzel, S. G. Mhaisalkar and A. C. Grimsdale, *J. Phys. Chem. C*, 2013, **117**, 15515–15522.
70 S. H. DuVall and R. L. McCreery, *Anal. Chem.*, 1999, **71**, 4594–4602.
71 K. Winkler, N. McKnight and W. R. Fawcett, *J. Phys. Chem. B*, 2000, **104**, 3575–3580.
72 Y. Fu, A. S. Cole and T. W. Swaddle, *J. Am. Chem. Soc.*, 1999, **121**, 10410–10415.
73 S. Yun, P. D. Lund and A. Hinsch, *Energy Environ. Sci.*, 2015, **8**, 3495–3514.
74 W. Lu, A. G. Fadeev, B. Qi, E. Smela, B. R. Mattes, J. Ding, G. M. Spinks, J. Mazurkiewicz, D. Zhou, G. G. Wallace, D. R. MacFarlane, S. A. Forsyth and M. Forsyth, *Science*, 2002, **297**, 983–987.
75 M. C. Goya, M. Lucero, A. Orive, A. Marín, Y. Gimeno, A. Creus, M. J. Aguirre, M. C. Arévalo and J. Armijo, *Int. J. Electrochem. Sci.*, 2011, **6**, 4984–4998.
76 M. Samadi Khoshkhoo, S. Maiti, F. Schreiber, T. Chassé and M. Scheele, *ACS Appl. Mater. Interfaces*, 2017, **9**, 14197–14206.
77 A. I. Martínez, L. Huerta, J. M. O. R. d. León, D. Acosta, O. Malik and M. Aguilar, *J. Phys. D: Appl. Phys.*, 2006, **39**, 5091.
78 H. Hantsche, *Adv. Mater.*, 1993, **5**, 778.
79 G. M. Rignanese, A. Pasquarello, J. C. Charlier, X. Gonze and R. Car, *Phys. Rev. Lett.*, 1997, **79**, 5174–5177.
80 A. Mohtasebi, T. Chowdhury, L. H. H. Hsu, M. C. Biesinger and P. Kruse, *J. Phys. Chem. C*, 2016, **120**, 29248–29263.